



Evaluation of corrosion resistance of Co-Cr alloys fabricated with different metal laser sintering systems

Süleyman Hakan Tuna¹, Erhan Karaca², İsmail Aslan³, Gürel Pekkan^{4*}, Nuran Özçiçek Pekmez²

¹Department of Prosthodontics, Faculty of Dentistry, Süleyman Demirel University, Isparta, Turkey

²Department of Chemistry, Faculty of Science, Hacettepe University, Ankara, Turkey

³Department of Prosthodontics, Faculty of Dentistry, Burdur Mehmet Akif Ersoy University, Burdur, Turkey

⁴Department of Prosthodontics, Faculty of Dentistry, Tekirdağ Namık Kemal University, Tekirdağ, Turkey

PURPOSE. The aim of this study was to evaluate the corrosion resistance of the specimens produced by five different commercial metal laser sintering (MLS) systems with their recommended Co-Cr alloy powders.

MATERIALS AND METHODS. The MLS machines and the alloy powders used were, ProX 100-ST2724G (St-Pro), Mysint 100-EOS SP2 (SP2-Mys), EOSINT 270-EOS SP2 (SP2-EOS), SLM 100-Starbond CoS (SB-SLM), and MLab Cusing-Remanium® Star (RS-MLab), respectively. Eight specimens from each group were prepared. Open circuit potential (E_{ocp}) and electrochemical impedance spectroscopy (EIS) measurements of polished surfaces of the specimens were conducted in a three-electrode cell using a potentiostat-galvanostat in Fusayama-Meyer artificial saliva (AS). Specimens from each group were immersed in AS and de-ionized water for seven days. E_{ocp} , charge transfer resistance (R_{ct}) values, and released ions ($\mu\text{g}/\text{cm}^2 \times 7\text{d}$) in different solutions were determined. The specimen surfaces were observed with SEM/EDS. Results were analyzed statistically. **RESULTS.** E_{ocp} values have shifted to potentials that are more positive over time. Steady-state E_{ocp} values were from high to low as follows, SB-SLM, SP2-Mys, SP2-EOS, RS-MLab, and ST-Pro, respectively. After 60 mins, RS-MLab specimens had the highest R_{ct} value, followed by SP2-Mys, SB-SLM, SP2-EOS, and ST-Pro. In all groups, ion release was higher in AS than that in de-ionized water. **CONCLUSION.** There were small differences among the corrosion resistances of the Co-Cr alloy specimens produced with MLS systems; meanwhile, the corrosion resistances were quite high for all specimens. [J Adv Prosthodont 2020;12:114-23]

KEYWORDS: Co-Cr alloy; Corrosion; Metal laser sintering; Powder

INTRODUCTION

Metals and metallic alloys have been used for hundreds of years in dentistry. Cobalt-chromium (Co-Cr) alloys have been preferred for a long time because of their high strength, hardness, corrosion resistance, and low cost.¹⁻³ Today, by

developments in additive manufacturing (AM) and laser technology, Co-Cr metallic dental prostheses or prosthetic parts are manufactured via three dimensional (3D) metal printers and metal laser sintering (MLS) systems that have become alternative to conventional casting methods.

Different laser sintering systems use the terms as selective laser sintering (SLS) or direct metal laser sintering (DMLS) and selective laser melting (cushing) (SLM) for the MLS process. SLS and DMLS terms express the same procedure. However, SLS used materials such as plastics, glass, and ceramics, whereas DMLS is attributed to the process applied to metal alloys. In this process, the powder is not fully melted. It is heated to the point that the powder granules can fuse on a molecular level. In SLM, the powder is fully melted. In metal alloys, there is no single melting point; there are, however, melting range. When working with metal alloys, it is claimed that the SLS or DMLS technique works better; however, when laser sintering pure titanium, the

Corresponding author:

Gürel Pekkan

Department of Prosthodontics, Faculty of Dentistry, Tekirdağ Namık Kemal University, Degirmenalti Yerleskesi, Namık Kemal Mah., Kampus Cad., No:1, 59030, Suleymanpasa, Tekirdağ, Turkey

Tel. +902822506303: e-mail, gpekkannku.edu.tr

Received August 23, 2019 / Last Revision March 14, 2020 / Accepted April 29, 2020

© 2020 The Korean Academy of Prosthodontics

This is an Open Access article distributed under the terms of the Creative Commons Attribution Non-Commercial License (<http://creativecommons.org/licenses/by-nc/4.0>) which permits unrestricted non-commercial use, distribution, and reproduction in any medium, provided the original work is properly cited.

SLM technique should be used. The parts fabricated with the SLM technique claimed to have fewer or no voids when using with a single metal powder. In this study, the term MLS is used for the laser sintering systems that sinter Co-Cr alloy powder.

MLS has various advantages over conventional methods. In this technique, different dental laboratory procedures such as waxing, investing, and casting are eliminated. Additionally, distortion of dental frameworks is prevented, and working time and the human-related (dental technician, clinician) errors are decreased. Nevertheless, high installation and equipment costs are the main disadvantages of this technology. However, the widespread use and the launching of different MLS systems have led to a decrease in costs.

In the MLS method, metal parts are produced directly by the AM technology, which is named as powder bed fusion. The standard tessellation language (STL) of the 3D computer-aided-design (CAD) model is used for data transfer to the MLS system. MLS system software receives the STL data, and the manufacturing begins with layer-by-layer production by fusing fine layers of metal powder by means of a high-power source of a focused laser beam. It uses the heat of a solid-state laser for sintering metal powders.⁴

In many studies, the corrosion behavior, microstructural and mechanical properties of laser-sintered, milled and cast Co-Cr alloys are investigated.^{2,3,5-11} Moreover, metal-porcelain bond strength, internal and marginal fit of Co-Cr copings fabricated with the cast, milled, and laser sintering methods were compared.^{7,10} Most of the studies revealed that laser sintering methods are superior to the other methods.

The corrosion resistance of metallic prostheses or the metallic prosthetic parts should be high enough to use them in extreme aggressive oral conditions. In corrosion, released metal ions cause deterioration of metallic alloys and produce adverse oral or systemic effects on patients. In the oral cavity, saliva and other external factors create a biochemical medium. Therefore, the chemical stability and corrosion resistance of the metallic parts of the dental prostheses made of different alloys are crucial factors for clinical success.¹²

MLS systems, which are widely used in dentistry in last decade, are fundamentally similar, but differ in their process parameters, such as laser power, scan speed, laser strategy,

specific powder, powder compacting method (with roller or recoater).²⁻¹² In addition, some properties of these systems are business secrets.¹³ However, each difference in production parameters can affect the product properties such as mechanical, microstructure, and corrosion resistance.

MLS system manufacturers claim to create more homogeneous, porosity-free, and corrosion-resistant structures when marketing their systems. In this study, the corrosion resistance of different MLS systems used for the fabrication of fixed dental prostheses and removable denture frameworks with their recommended Co-Cr-based powders are evaluated.

MATERIALS AND METHODS

A total of 40 cylindrical Co-Cr specimens, 4 mm in diameter, 30 mm in height, were produced with five different MLS systems. All of the specimens were fabricated layer-by-layer vertically, starting from the bottom of the cylinder. The general properties and process parameters of the systems are shown in Table 1. Co-Cr alloy powders and their contents are shown in Table 2. The Co-Cr powders used were system-specific or the powders recommended by the MLS system manufacturers.

After production, all specimens were sandblasted with 50 μm Al_2O_3 and applied heat treatment according to the manufacturers' recommendations. The finishing and polishing procedures were performed on one flat-end surface of the cylinder using light pressure under standard conditions with a high-speed polishing machine. Metallographic polishing procedure was completed with 1- μm diamond paste and the specimens were cleaned with ethanol in ultrasonic bath for 5 min.¹ For each of the three electrodes, to be used as electrodes for electrochemistry tests, 2 mm-thick, 6 cm-long copper wire was soldered to one end. Epoxy resin was used to coat the specimens, excluding their polished surfaces and the tip of copper wires to be used as an electrode. The surface area of the electrode of the specimens was as 12.56 mm^2 .

All electrochemical measurements were conducted in a 25 mL lactic acid buffered artificial saliva solution (AS) (Fusayama-Meyer, Chromatographic Specialties Inc., Brockville, Canada)

Table 1. MLS machines with their technical information

	Machine (Model)	Laser (Source)	W	Layer thickness (μm)	Laser spot diameter (μm)	Scanning speed (m/s)
1	ProX 100	Fiber	50	20	28	2
2	Mysint 100	Fiber	90	20	50	8
3	EOSINT M 270	Yb-Fiber	185	20	200	2
4	SLM 100	Fiber	100	20	28	0.2
5	MLab Cusing	Fiber	100	20	50	2

1. 3D SYSTEMS (Riom, France), 2. SISMA SpA (Rocchette, Italy), 3. EOS GmbH (Munich, Germany), 4. Realizer GmbH (Borchen, Germany), 5. Concept Laser GmbH (Lichtenfels, Germany).

Table 2. The chemical composition of the commercial Co-Cr alloy powders and coding of the systems (machine + powder)

N	Powder Code	Element (% of weight)						MLS (Machine)	System (Machine+ Powder)
		Co	Cr	Mo	W	Si	Others		
1	ST	Balance	28 - 30	5 - 6	-	0 - 1	Mn 0 - 1; Fe 0 - 0.5; C 0 - 0.02	ProX 100	ST-Pro
2	SP2	61.8	23.7	4.6	4.9	0.8	Fe max 0.5; Mn max 0.1	Mysint 100	SP2-Mys
3	SP2	61.8	23.7	4.6	4.9	0.8	Fe max 0.5; Mn max 0.1	EOSINT M 270	SP2-EOS
4	SB	59	25	3.5	9.5	1	(C + Fe + Mn + N) < 1	SLM 100	SB-SLM
5	RS	60.5	28	-	9	1.5	(Mn + N + Nb + Fe) < 1	MLab Cusing	RS-MLab

The coding was done according to the name of the laser sintering machine and the specific powder used in the production of each specimen group.

ST: ST2724G; Sint-tech, Riom, France. LOT: 16D0296

SP2: EOS SP2; Turku, Finland. LOT: H301601

SB: Starbond CoS S&S; Scheffner GmbH, Mainz, Germany. LOT: 019020817

RS: Remanium® star; Dentaaurum, Ispringen, Germany. LOT: 474975A

with a pH of 5.3, at 37°C which was open to atmosphere.¹ Before each experiment, the AS was refreshed. It was composed of 1.000 g urea; 0.906 g CaCl₂·2H₂O; 0.690 g NaH₂PO₄·2H₂O; 0.400 g KCl; 0.400 g NaCl; 0.005 g Na₂S₂O₈·9H₂O (Sigma Chemical Co., St. Louis, MO, USA). The solution was diluted with deionized water to 1000 mL.

Electrochemical measurements were performed in a three-electrode cell using CHI-6011D potentiostat for three specimens from each group. The prepared electrodes (0.126 cm²), saturated calomel electrode (SCE), and platinum foil were used as working, reference and counter electrodes, respectively. The working electrodes were held in AS's to determine the steady-state of open circuit potential (E_{ocp}) values for 10 hours (Fig. 1).

The electrochemical impedance spectroscopy (EIS) was performed for all specimens in AS (25 mL). EIS measurements were carried out using AS (25 mL) with an amplitude of 5 mV, within a frequency range from 10⁵ to 10⁻² Hz at the E_{ocp} of the substrates. The Nyquist (Fig. 2) and Bode (Fig. 3) plots for each specimen were recorded, and the

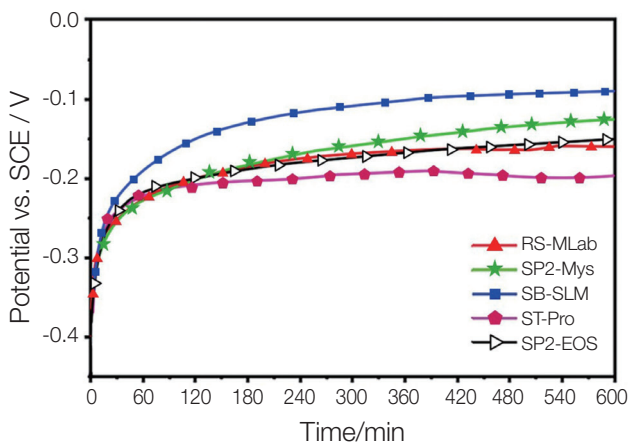


Fig. 1. E_{ocp} curves for 10 hours.

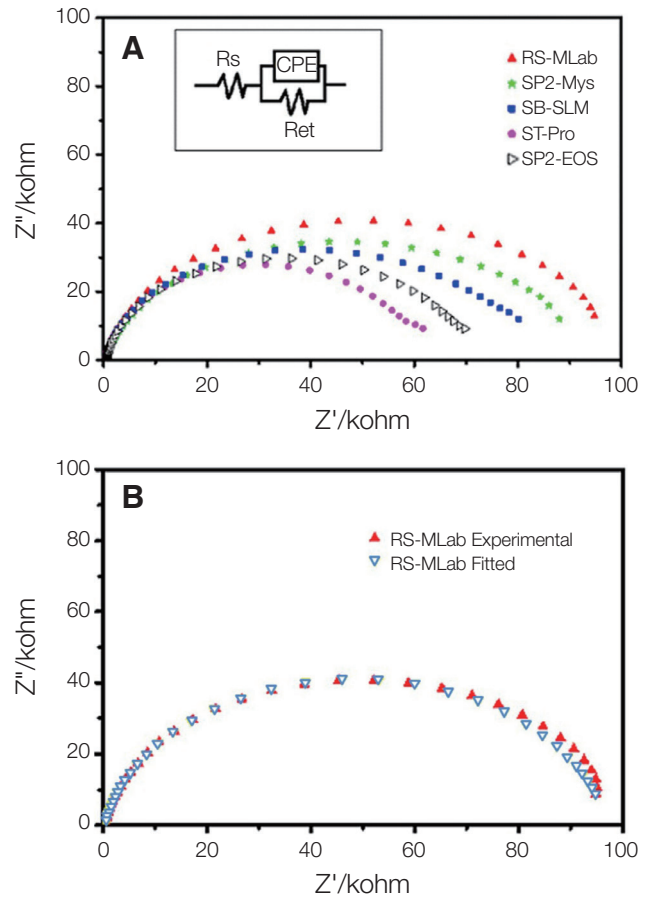


Fig. 2. (A) Nyquist plots of specimens recorded in artificial saliva solution and equivalent circuit model based on EIS measurements of data obtained, (B) Experimental (red dotted) and fitted (yellow dotted) data for the Nyquist curve of RS-MLab.

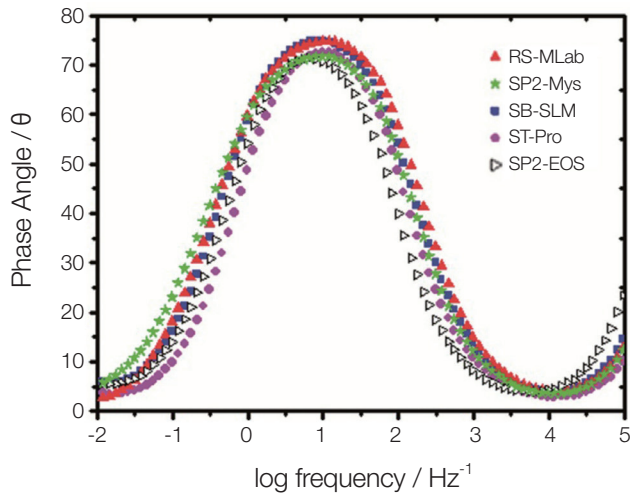


Fig. 3. Bode plots of specimens recorded in artificial saliva solution.

average behavior of each repeated group was plotted. The diameter of the semicircle in Nyquist plot shows the charge transfer resistance (R_{ct}), and the specimen with the largest semicircle corresponds to the most corrosion-resistant one (Fig. 2A). The semicircle diameter corresponds to equivalent circuit models, which were generated using software (ZsimpWin V350, AMETEK, Berwyn, IL, USA) based on the data obtained by EIS measurements. In Fig. 2A, the equivalent circuit model utilized for all specimens is shown. In Fig. 2B, it is shown that the experimental Nyquist impedance curves were fitted well to this equivalent circuit model. The R_{ct} s obtained by fitting the impedance data corresponds to one of the circuit elements.

The static immersion test in polypropylene tubes was applied to three specimens from each group. The 12.56 mL de-ionized water and Fusayama-Meyer AS were used as an electrolyte solution, respectively. Polished specimens were

stored in the sealed tube at 37°C for 7 days. The released ions were determined as ppb ($\mu\text{g/L}$) using inductively coupled-plasma mass spectrometry (ICP-MS) (X SERIES 2, Thermo Fischer Scientific, Bremen, Germany).

Surface microstructures were analyzed by a scanning electron microscope (SEM) (NOVA Nanosem 650, FEI, Eindhoven, Netherlands). Two polished specimens from each group were examined. The specimens were also exposed to energy-dispersive X-ray spectroscopy (EDS) analysis (EDAX Inc., AMETEK Inc., Berwyn, IL, USA). After immersion, the specimen surfaces were subjected to SEM evaluation.

After SEM examination of the specimens, they were re-polished and etched for 30 seconds at room temperature with hydrochloric acid/hydrogen peroxide (80:20, v/v) (Sigma Chemical Co., St. Louis, MO, USA). Etched specimens were again examined by using SEM.

Results were analyzed statistically using the SPSS software (SPSS/PC, Vers. 23; SPSS, Chicago, IL, USA). The results of the E_{ocp} , $R_{ct}/\Omega \text{ cm}^2$, and total released ion amount ($\mu\text{g}/\text{cm}^2 \times 7 \text{ d}$) of the groups were subjected to repeated measurements of analysis of variance (ANOVA) at separate factorial level. Tukey's test was used to determine the difference between factor level means.

RESULTS

The E_{ocp} values of specimens changed rapidly up to one hour. There was a gradual increase in E_{ocp} values during the first two to three hours upon insertion into the solution. The potential of all samples became relatively stable at about -0.2 V (vs. SCE) after six hours due to a slowly forming unstable oxide layer. The E_{ocp} values shifted to more positive potentials in SB-SLM, SP2-Mys, SP2-EOS, RS-MLab, and ST-Pro, leading to more protection resistance (Table 3).

As a result of the ANOVA calculated from the data obtained in terms of E_{ocp} values, time \times specimen group interaction was found to be statistically significant ($P < .05$).

Table 3. Open circuit potential (E_{ocp}) values at 15, 60 minutes, and steady-state (Mean \pm SD)

Specimen	E_{ocp} 15 min	E_{ocp} 60 min	E_{ocp} steady state
ST-Pro	-0.243 \pm 0.020 ^{Ca}	-0.210 \pm 0.010 ^{Bb}	-0.176 \pm 0.011 ^{Ac}
SP2-Mys	-0.220 \pm 0.060 ^{Ca}	-0.183 \pm 0.032 ^{Bab}	-0.126 \pm 0.020 ^{Ab}
SP2-EOS	-0.240 \pm 0.030 ^{Ca}	-0.193 \pm 0.015 ^{Bb}	-0.143 \pm 0.030 ^{Abc}
SB-SLM	-0.230 \pm 0.040 ^{Ca}	-0.140 \pm 0.070 ^{Ba}	-0.050 \pm 0.104 ^{Aa}
RS-MLab	-0.220 \pm 0.060 ^{Ca}	-0.183 \pm 0.035 ^{Bab}	-0.143 \pm 0.020 ^{Abc}
Time \times specimen group interaction	F = 3.446 P = .0121		
Time	F = 89.015 P = .000		
Specimen	F = 1.231 P = .364		

Different superscript capital letters mean a statistically significant difference among times in each system, and different lower-case superscript letters mean a statistically significant difference among the systems at each time, according to Tukey's tests.

This means that in each specimen group and among specimen groups, the difference between the E_{ocp} values changes over time. According to these results, Tukey's tests were performed, as shown in Table 3.

After 15 minutes, SP2-EOS and RS-MLab had the highest and the lowest R_{ct} value, respectively. After 1 hour, the RS-MLab and ST-Pro reached the highest and the lowest R_{ct} values, respectively (Table 4).

Time \times specimen group interaction was also found to be statistically significant as a result of the ANOVA of the data obtained in terms of R_{ct}/Ω cm² values ($P < .01$). After 15 min, the values of the SP2-EOS were greater than those of the ST-Pro, SP2-Mys, and RS-MLab. Hence, there was no statistically significant difference among the mean values of the ST-Pro, SP2-Mys, SB-SLM, and RS-MLab ($P > .05$). After one hour, there was a statistically significant difference among groups ($P < .05$), and RS-MLab had the highest values, followed by SP2-Mys, SB-SLM, SP2-EOS, and ST-Pro (Table 4).

Table 4. R_{ct}/Ω cm² values at 15 minutes and 60 minutes (Mean \pm SD)

Specimen	R_{ct}/Ω cm ² (15 min)	R_{ct}/Ω cm ² (1 h)
ST-Pro	3640 \pm 360 ^{Bb}	4530 \pm 223 ^{Ad}
SP2-Mys	3550 \pm 304 ^{Bb}	6313 \pm 130 ^{Ab}
SP2-EOS	4160 \pm 819 ^{Ba}	5090 \pm 144 ^{Ac}
SB-SLM	3813 \pm 924 ^{Bab}	5843 \pm 178 ^{Ab}
RS-MLab	3350 \pm 156 ^{Bb}	7053 \pm 195 ^{Aa}
Time \times specimen group interaction	F = 14.989	P = .000
Time	F = 218.465	P = .000
Specimen	F = 4.374	P = .027

The amount of ion released in de-ionized water is shown in Table 5. According to the results of the ANOVA, the specimen group \times solution interaction was not statistically significant ($P > .05$). However, the amount of ion released from all specimen groups in the AS was higher than that in de-ionized water. The total mean ion release among groups was statistically significantly different ($P < .05$). The highest total mean ion release was in St-Pro specimens. According to the results of the Tukey's tests, the total mean ion release between ST-Pro and RS-MLab specimens were statistically significantly different ($P < .05$).

As seen in Table 6, according to the results of EDS analysis, weight percentages of the elements on the surface of the specimens were almost the same as those found in the composition of the alloys. In Fig. 4, SEM micrographs of the polished, immersed, and etched surfaces of the specimens are seen. Fine-grained particles are detected on polished surfaces. On the etched surfaces, superficial abrasion and fine particles were observed. In addition, etching of the alloy surfaces, as well as immersion in different solutions, did not affect the surface morphology of the specimens. Porosities were seen on all specimen surfaces.

DISCUSSION

The quality and the properties of resultant product obtained from MLS method are affected from many factors, such as laser power, scan speed, line spacing, strategy of processing and heat treatment.¹⁴ The composition of the Co-Cr alloy powder used and the particle size distribution of the powder may also influence the properties or the quality of the product obtained.¹⁴ Therefore, some MLS device manufacturers do not recommend or accept some Co-Cr alloy powders to be used with their devices. They only support the production with a certain particle size range and recommended alloy powders. For that reason, each brand of

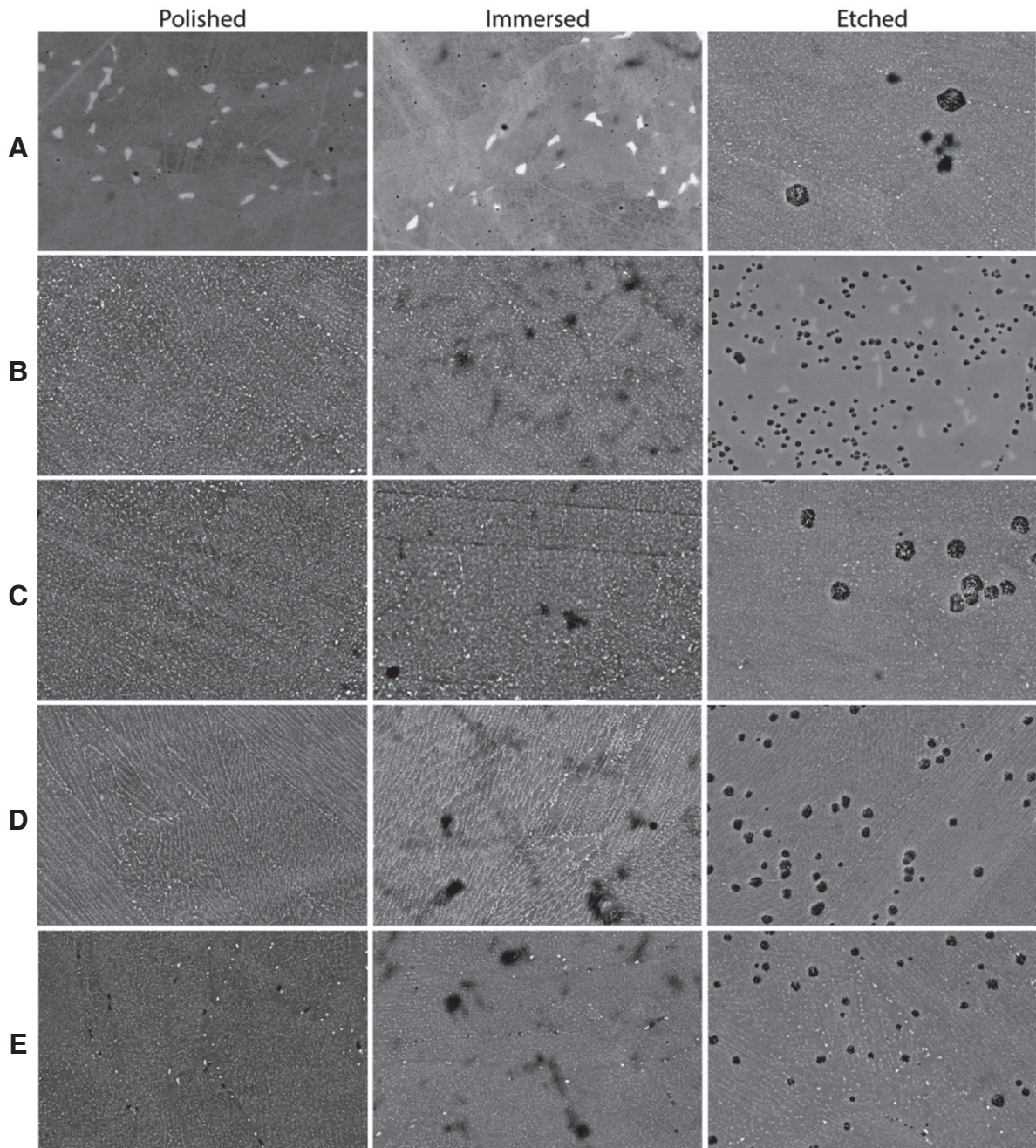
Table 5. ICP-MS results of total ion release from specimens (Mean \pm SD)

Total of the released ions ($\mu\text{g}/\text{cm}^2 \times 7$ d)			
Specimen	De-ionized water	Artificial saliva	Total mean
ST-Pro	0.830 \pm 0.380	1.350 \pm 0.851	1.090 ^A
SP2-Mys	0.504 \pm 0.253	1.094 \pm 0.253	0.799 ^{AB}
SP2-EOS	0.794 \pm 0.318	1.129 \pm 0.622	0.962 ^{AB}
SB-SLM	0.770 \pm 0.377	1.040 \pm 0.692	0.905 ^{AB}
RS-MLab	0.463 \pm 0.172	1.074 \pm 0.358	0.769 ^B
Total mean	0.6722 ^B	1.1374 ^A	
Specimen group \times solution interaction	F = 1.137	P = .367	
Specimen group	F = 3.037	P = .041	
Solution	F = 49.02	P = .000	

Different superscript capital letters mean a statistically significant difference between total means in each solution, according to Tukey's tests.

Table 6. Results of the EDS in weight %

Specimen	Element (weight %)					
	Co	Cr	Mo	W	Si	Others
ST-Pro	61.78	31.54	2.96	-	0.23	Mn: 2.04
SP2-Mys	63.31	25.98	3.84	5.87	1	
SP2-EOS	63.02	26.48	3.82	5.82	0.86	
SB-SLM	57.39	26.05	3.34	11.49	1.01	Fe: 0.62; Mn: 0.1
RS-MLab	60.16	28.97	-	8.62	1.48	Fe: 0.30; Mn: 0.45

**Fig. 4.** SEM view of polished, immersed, and etched specimens from each group. (A) ST-Pro, (B) SP2-Mys, (C) SP2-EOS, (D) SB-SLM, (E) RS-MLab (Magnification $\times 10,000$).

Co-Cr alloy powders could not be tested in each MLS device. In this study, widely used MLS machines, and powders recommended by manufacturers of these machines were selected, and the MLS device and its respective powder was considered as a whole system.

In the present study, the corrosion resistance of five MLS systems was compared. The E_{ocp} values obtained from RS-MLab, SP2-Mys, ST-Pro, SB-SLM, and SP2-EOS alloys treated with AS were plotted as functions of the immersion time in Fig. 1. There was a gradual increase in E_{ocp} during the first two to three hours upon insertion into the solution. The potential of all specimens became relatively stable at about -0.2 V (vs. SCE) after six hours because of the slowly forming unstable oxide layer. E_{ocp} values shifted to more positive potentials in SB-SLM, SP2-Mys, SP2-EOS, RS-MLab, and ST-Pro specimens, leading to more protection resistance. The ST-Pro produced a lower potential oxide layer but was not as stable as the others. Galo *et al.*¹⁵ indicated that for the determination of corrosion resistance of dental alloys, it would not be sufficient solely to consider the E_{ocp} . Therefore, in this study, the EIS technique was also used to evaluate the corrosion characteristics of the materials. The application of a time-varying voltage and current response measurement are included in the EIS technique. The ratio of two gives the frequency-dependent impedance.¹⁶ It has been demonstrated that EIS is a superior method to characterize corrosion characteristics of metal specimens with surface oxide films.¹⁷ Regarding resistance properties of materials that have similar compositions, more precise information can be achieved with EIS. A material that has a high resistance to corrosion is expected to have a high R_{ct} value. In this study, R_{ct} values after 15 minutes were found in similar range. After one hour, EIS results (and R_{ct} values) of all specimens were close to each other. The highest R_{ct} value was 7053 Ωcm^2 in RS-MLab group, and the lowest R_{ct} value was 4530 Ωcm^2 in the ST-Pro group. Accordingly, the surface of the RS-MLab specimens appeared to form a more stable corrosion-resistant oxide layer. Considering E_{ocp} and EIS results, a less stable and unstable oxide layer of the ST-Pro specimens may result from the composition of the alloy powder used.

The corrosion resistance of a Co-Cr alloy increase as the proportion of Cr reaches 25%.¹ Corrosion resistance depends on the production of passive films on Co alloys. In Co-Cr alloys, corrosion resistance increases due to the passivation effect of the Cr oxide layer covering the surface.^{18,19} In this study, Cr is more than 25% in both ST-Pro and RS-MLab specimens and 25% in SB-SLM specimens. Tungsten (W) serves as an intermetallic compound and helps increase corrosion resistance by the formation of Cr-depleted zones.²⁰ By forming the Co_3Mo (hcp) intermetallic compound, molybdenum (Mo) improves the corrosion resistance. Mo also acts as a solid-solution strengthener.²¹ In this study, there is 9% W in the composition of RS-MLab, and there is no Mo. There is 5 - 6% Mo and 0% W in the composition of ST-Pro. In a previous study, Tuna *et al.*¹ found that the corrosion resistance of Co-Cr alloys with

low W content was also low. A small compositional change about these elements mentioned above in the alloy may alter the corrosion behavior of the material.²² Although SP2-Mys and SP2-EOS specimens were produced from the same alloy powder, in this study, small differences in their E_{ocp} and EIS values were found. These differences might be caused by the difference in the MLS system or operating parameters.

Tuna *et al.*¹ revealed that the corrosion resistance of Co-Cr specimens produced by laser sintering was higher than that of cast ones, and R_{ct} values of laser-sintered specimens were up to twenty times higher than those of cast specimens. However, in this study, only Co-Cr specimen groups obtained by laser sintering were compared; thus, the range of difference among them was small. Although there were small differences among both E_{ocp} and $R_{ct} / \Omega\text{cm}^2$ values of the specimen groups, it can be stated that all specimen groups have high corrosion resistance and met the requirements for dental restoration materials (ISO 22674: 2016, Dentistry - Metallic materials for fixed and removable restorations and appliance).

Clinically, possession of minimal ion release is expected from an ideal alloy.^{23,24} The corrosion resistance of a metal or an alloy depends not only on its own properties but also on its interactions with surrounding structures.^{25,26} An alloy may exhibit different corrosion resistance in different solutions or biological environment.²⁷ In this study, immersion tests were performed in Fusayama-Meyer AS and in de-ionized water. In Fusayama-Meyer AS, the total amount of ions released was almost two times higher than that in de-ionized water (Table 5). Lu *et al.*² reported that in phosphate buffered saline (PBS) solution, approximately 0.22 $\mu\text{g}/\text{cm}^2/7\text{d}$ Co was released from laser sintered Co-Cr-W alloy. But in a similar study,¹¹ the immersion test in PBS solution resulted in 0.45 $\mu\text{g}/\text{cm}^2/7\text{d}$ Co release from laser-sintered Co-Cr-Mo alloy. In this study, there was a significant difference between the total amount of ions released from St-Pro specimens and RS-MLab in both Fusayama-Meyer AS and de-ionized water (Table 5). In different solutions, the amount of ion release was changed. When released ions were examined, it was determined that the maximum amount of Co was released compared to the other elements. The released amounts of Cr, W, and Mo were either too little or were not measurable. In previous studies, it was stated that the most released element was Co from both laser-sintered Co-Cr-W and Co-Cr-Mo alloy.^{2,13,28}

Metal ions released from an alloy influence the microstructure and composition of the material, the nature and strength of the metal-oxide bond, the thickness of oxide films, and the role of alloying element.^{25,29,30} Some elements involved in biological functions such as Zn, Cu, Ni, Co, Mo, and Cr released from dental alloys cannot exceed the daily dietary intake level.³¹ The daily dietary intake of Co, Cr, and Mo is 250 μg , 240 μg , and 400 μg , respectively.³²

The corrosion behavior of a material significantly affects the mechanical properties and biocompatibility.³³ It is also correlated with several factors, such as the manufac-

turing process and the alloying elements.³⁴ Studies have shown that leaching of metal ions from Co-Cr-Mo orthopedic implants can cause various diseases, and the addition of calcium phosphate (CaP) to this alloy was found to be effective in reducing ion release and in increasing abrasion resistance.^{26,27} In the present study, the maximum total ion release from the specimens was 0.830 $\mu\text{g}/\text{cm}^2/7\text{d}$ in de-ionized water and 1.350 $\mu\text{g}/\text{cm}^2/7\text{d}$ in Fusayama-Meyer AS. These amounts are similar compared with the literature findings.^{13,35} The total amount of ion released is well below the standard of EN ISO 10271, 200 $\mu\text{g}/\text{cm}^2/7\text{d}$.¹ Xin *et al.*³⁶ showed that Co-Cr specimens fabricated by MLS had lower metal ion release, higher corrosion resistance, and lower cell proliferation in comparison with the cast Co-Cr alloy specimens that was attributed to the formation of fine microstructure with cellular dendrites during the material's rapid solidification.

Porosity deteriorates the mechanical properties of a material. It is undesirable in the microstructure because it causes pitting and crevice corrosion and increases susceptibility to corrosion on the entire material surface.³⁷ Takaichi *et al.*⁹ stated that there was a strong correlation between the operational parameters such as scan spacing and laser power of the MLS devices and the porosity, microstructure, and mechanical properties of the sintered alloy. In the MLS technique, it is theoretically accepted that alloys are produced up to 100% nominal density. However, this depends on the very appropriate adjustment of the operating conditions, such as laser power, scan thickness, scan spacing, and the scan rate.²⁴

The MLS molding process is a rapid melting and solidification procedure. This process reduces porosities and flaws, and a homogenous and small-grained dense material can be obtained.³⁸ Generally, the final product is heat-treated for enhancing the microstructural and mechanical properties. Heat treatment is needed for the elimination of crystal defects such as dislocations in alloys and consequently for stabilization of microstructure and reduction of residual stresses.³⁹

MLS technique is claimed to be superior to conventional casting technique as it allows the fabrication of objects with enhanced mechanical properties even in complex geometries and very fine microstructures.⁴⁰ Fast cooling in the MLS technique provides smaller grains compared to slow cooling process in conventional casting. In different studies, it was shown that Co-Cr alloys fabricated by the SLM technique possessed much finer grains and superior mechanical properties when compared with the casting technique.^{6,17} Moreover, a much finer and non-equilibrium structure could be seen in SLM groups with a grain size of 2 - 20 μm .⁷

The MLS process starts with laser irradiation on the metal powders, and a molten pool is formed. Each molten layer (~1400°C) is rapidly cooled down to the preheated bed temperature of approximately 200°C. The designed structure is produced layer-by-layer according to layer thickness information of the system. The final performance of the built structure is determined by the shape and continuity

of the pool. In a recent study, it was revealed that the geometry of the molten pool affected the properties of the Co-Cr alloys and the morphology of the molten pool was associated with laser power, scanning line spacing, and sweeping speed.⁴¹

In the MLS process, melting temperature, laser beam absorption/reflection coefficients, and thermal conductivity properties of an alloy should be evaluated for adjusting the operational parameters. In reference to Co-Cr dental alloys, these data are well known and remain unchanged. However, the average grain diameter of the powder brand used would affect mechanical properties and other metallurgical phenomena during solidification.^{9,39} In the current study, although SP2-Mys and SP2-EOS specimens were produced from the same alloy powder, there was a difference in their E_{ocp} and R_{ct} values. The powder supplied from the powder dispenser is affected by splashes in laser scanning. Some powder particles may be fused by the laser beam, and in the case of laying a new layer of powder, the fused grains in the powder bed may affect the sintering quality of the material. Therefore, after each laser sintering process, it is important to ensure that the powders, remaining on the top of the powder dispenser and in the powder bed are collected and sieved by means of a special vacuum cleaner to guarantee powder quality standardization.

Instrument settings affect the sintering procedure and the quality of the final product. These settings cover heating rate, holding time, and the temperature of the preheated bed, as well as scan speed and layer thickness.^{9,42} The layer thickness of the first manufactured SLM systems was about 50 to 80 μm . The developments on the machines enabled the production of layer thicknesses as 20 μm in dental applications.⁴²

The overall corrosion behavior of an alloy is correlated with the elemental composition and distribution in the material, and it is strongly affected by the segregation of alloying elements in the microstructure.²² In the Co-Cr specimens obtained by the casting method, the overall ratio of the elements in the alloy surfaces and the general content of the material are not similar.²⁸ In addition, the distribution of the elements in the surface and the interior of the material may also be different. In this study, according to the results of EDS analysis, the percentages of the elements in the surface of the samples were found to be almost the same as the element ratios in the content of the alloy. The microstructural heterogeneities could act as an initiating site for preferential corrosion.⁴³ In the current study, in SEM images, fine homogeneous particles were observed (Fig. 4). Differences between the laser W power of the devices, the contents of the powders used, and the differences in particle size distributions may have affected the results of this study.

CONCLUSION

There were small differences among the corrosion resistances of the Co-Cr alloy specimens produced with MLS

systems in this study. The corrosion resistance of all specimens was found to be quite high and met the requirements for dental restoration materials. In AS solution, the ion release was higher than that in de-ionized water. The differences might be due to the contents of the alloys used, the particle sizes of the powders, and other reasons such as operating parameters.

ORCID

Süleyman Hakan Tuna <https://orcid.org/0000-0002-8305-1086>

Erhan Karaca <https://orcid.org/0000-0002-9100-8870>

İsmail Aslan <https://orcid.org/0000-0003-2822-6979>

Gürel Pekkan <https://orcid.org/0000-0003-4361-8639>

Nuran Özçiçek Pekmez <https://orcid.org/0000-0002-7223-790X>

REFERENCES

1. Tuna SH, Özçiçek Pekmez N, Kürkçüoğlu I. Corrosion resistance assessment of Co-Cr alloy frameworks fabricated by CAD/CAM milling, laser sintering, and casting methods. *J Prosthet Dent* 2015;114:725-34.
2. Lu Y, Wu S, Gan Y, Li J, Zhao C, Zhuo D, Lin J. Investigation on the microstructure, mechanical property and corrosion behavior of the selective laser melted CoCrW alloy for dental application. *Mater Sci Eng C Mater Biol Appl* 2015;49:517-25.
3. Davis JR. ASM specialty handbook: Nickel, cobalt, and their alloys. ASM International; USA: 2000. p. 343-401.
4. Simchi A. Direct laser sintering of metal powders: Mechanism, kinetics and microstructural features. *Mater Sci Eng A Struct Mater* 2006;428:148-58.
5. Mumtaz KA, Erasenthiran P, Hopkinson N. High density selective laser melting of Waspaloy®. *J Mater Process Technol* 2008;195:77-87.
6. Zhou Y, Li N, Yan J, Zeng Q. Comparative analysis of the microstructures and mechanical properties of Co-Cr dental alloys fabricated by different methods. *J Prosthet Dent* 2018; 120:617-23.
7. Han X, Sawada T, Schille C, Schweizer E, Scheideler L, Geisgerstorfer J, Rupp F, Spintzyk S. Comparative analysis of mechanical properties and metal-ceramic bond strength of Co-Cr dental alloy fabricated by different manufacturing processes. *Materials (Basel)* 2018;11:1801.
8. Ucar Y, Akova T, Akyil MS, Brantley WA. Internal fit evaluation of crowns prepared using a new dental crown fabrication technique: laser-sintered Co-Cr crowns. *J Prosthet Dent* 2009; 102:253-9.
9. Takaichi A, Suyalatu, Nakamoto T, Joko N, Nomura N, Tsutsumi Y, Migita S, Doi H, Kurosu S, Chiba A, Wakabayashi N, Igarashi Y, Hanawa T. Microstructures and mechanical properties of Co-29Cr-6Mo alloy fabricated by selective laser melting process for dental applications. *J Mech Behav Biomed Mater* 2013;21:67-76.
10. Wang H, Feng Q, Li N, Xu S. Evaluation of metal-ceramic bond characteristics of three dental Co-Cr alloys prepared with different fabrication techniques. *J Prosthet Dent* 2016; 116:916-23.
11. Qian B, Saeidi K, Kvetková L, Lofaj F, Xiao C, Shen Z. Defects-tolerant Co-Cr-Mo dental alloys prepared by selective laser melting. *Dent Mater* 2015;31:1435-44.
12. Wataha JC. Alloys for prosthodontic restorations. *J Prosthet Dent* 2002;87:351-63.
13. Hedberg YS, Qian B, Shen Z, Virtanen S, Wallinder IO. In vitro biocompatibility of CoCrMo dental alloys fabricated by selective laser melting. *Dent Mater* 2014;30:525-34.
14. Hong MH, Min BK, Kwon TY. The influence of process parameters on the surface roughness of a 3D-printed Co-Cr dental alloy produced via selective laser melting. *Appl Sci* 2016;6:401.
15. Galo R, Ribeiro RF, Rodrigues RC, Rocha LA, de Mattos Mda G. Effects of chemical composition on the corrosion of dental alloys. *Braz Dent J* 2012;23:141-8.
16. Frankel GS. Electrochemical techniques in corrosion: status, limitations, and needs. *J Test Eval* 2008;42:517-38.
17. Xin XZ, Chen J, Xiang N, Gong Y, Wei B. Surface characteristics and corrosion properties of selective laser melted Co-Cr dental alloy after porcelain firing. *Dent Mater* 2014;30:263-70.
18. McCabe JF, Walls AWG. Applied dental materials. 9th ed. Oxford: Blackwell Publishing Ltd.; UK: 2008. p. 4-84.
19. Schmalz G, Garhammer P. Biological interactions of dental cast alloys with oral tissues. *Dent Mater* 2002;18:396-406.
20. Viennot S, Dalard F, Lissac M, Grosgeat B. Corrosion resistance of cobalt-chromium and palladium-silver alloys used in fixed prosthetic restorations. *Eur J Oral Sci* 2005;113:90-5.
21. Shin JC, Doh JM, Yoon JK, Lee DY, Kim JS. Effect of molybdenum on the microstructure and wear resistance of cobalt-base Stellite hardfacing alloys. *Surf Coat Technol* 2003; 166:117-26.
22. Matković T, Matković P, Malina J. Effects of Ni and Mo on the microstructure and some other properties of Co-Cr dental alloys. *J Alloys Compd* 2004;366:293-7.
23. Ren L, Memarzadeh K, Zhang S, Sun Z, Yang C, Ren G, Allaker RP, Yang K. A novel coping metal material CoCrCu alloy fabricated by selective laser melting with antimicrobial and antibiofilm properties. *Mater Sci Eng C Mater Biol Appl* 2016;67:461-7.
24. Siddharth R, Gautam R, Chand P, Agrawal KK, Singh RD, Singh BP. Quantitative analysis of leaching of different metals in human saliva from dental casting alloys: An in vivo study. *J Indian Prosthodont Soc* 2015;15:206-10.
25. Bergman M. Corrosion in the oral cavity--potential local and systemic effects. *Int Dent J* 1986;36:41-4.
26. Sahasrabudhe H, Bose S, Bandyopadhyay A. Laser processed calcium phosphate reinforced CoCrMo for load-bearing applications: Processing and wear induced damage evaluation. *Acta Biomater* 2018;66:118-28.
27. Bandyopadhyay A, Shivaram A, Isik M, Avila JD, Dernell WS, Bose S. Additively manufactured calcium phosphate reinforced CoCrMo alloy: Bio-tribological and biocompatibility evaluation for load-bearing implants. *Addit Manuf* 2019;28: 312-24.
28. Hodgson AWE, Kurz S, Virtanen S, Fervel V, Olsson COA, Mischler S. Passive and transpassive behaviour of CoCrMo in

- simulated biological solutions. *Electrochim Acta* 2004;49: 2167-78.
29. Okazaki Y, Gotoh E. Comparison of metal release from various metallic biomaterials in vitro. *Biomater* 2005;26:11-21.
 30. Tuna SH, Pekmez NÖ, Keyf F, Canli F. The influence of the pure metal components of four different casting alloys on the electrochemical properties of the alloys. *Dent Mater* 2009;25: 1096-103.
 31. López-Álías JF, Martínez-Gomis J, Anglada JM, Peraire M. Ion release from dental casting alloys as assessed by a continuous flow system: Nutritional and toxicological implications. *Dent Mater* 2006;22:832-7.
 32. Wataha JC. Biocompatibility of dental casting alloys: a review. *J Prosthet Dent* 2000;83:223-34.
 33. Valero Vidal C, Igual Munoz A. Study of the adsorption process of bovine serum albumin on passivated surfaces of CoCrMo biomedical alloy. *Electrochim Acta* 2010;55:8445-52.
 34. Liverani E, Fortunato A, Leardini A, Belvedere C, Siegler S, Ceschini L, Ascari A. Fabrication of Co-Cr-Mo endoprosthetic ankle devices by means of Selective Laser Melting (SLM). *Mater Design* 2016;106:60-8.
 35. Kettelaraj JA, Lidén C, Axén E, Julander A. Cobalt, nickel and chromium release from dental tools and alloys. *Contact Dermatitis* 2014;70:3-10.
 36. Xin XZ, Xiang N, Chen J, Wei B. In vitro biocompatibility of Co-Cr alloy fabricated by selective laser melting or traditional casting techniques. *Mater Lett* 2012;88:101-3.
 37. Muñoz AI, Mischler S. Effect of the environment on wear ranking and corrosion of biomedical CoCrMo alloys. *J Mater Sci Mater Med* 2011;22:437-50.
 38. Kurz W, Fisher DJ. *Fundamentals of solidification*. 3rd ed. Aedermannsdorf: Trans Tech Publications; Switzerland: 1989. p. 1-15.
 39. Kruth JP, Mercelis P, Van Vaerenbergh J, Froyen L, Rombouts M. Binding mechanisms in selective laser sintering and selective laser melting. *Rapid Prototyp J* 2005;11:26-36.
 40. Prashanth K, Scudino S, Klauss H, Surreddi KB, Lober L, Wang Z, Chaubey A, Kuhn U, Eckert J. Microstructure and mechanical properties of Al-12Si produced by selective laser melting: Effect of heat treatment. *Mater Sci Eng A* 2014;590: 153-60.
 41. Standard specification for cobalt-28 chromium-6 molybdenum alloy castings and casting alloy for surgical implants. ASTM International; West Conshohocken, PA, USA: 2012. ASTM F75-12.
 42. Koutsoukis T, Zinelis S, Eliades G, Al-Wazzan K, Rifaiy MA, Al Jabbari YS. Selective laser melting technique of Co-Cr dental alloys: A review of structure and properties and comparative analysis with other available techniques. *J Prosthodont* 2015;24:303-12.
 43. Montero-Ocampo C, Juarez R, Rodriguez AS. Effect of fcc-hcp phase transformation produced by isothermal aging on the corrosion resistance of a Co-27Cr-5Mo-0.05C alloy. *Metall Mater Trans A* 2002;33:2229-35.